Plug-and-Play Robust Voltage Control of DC Microgrids

Mahdieh S. Sadabadi, Qobad Shafiee, and Alireza Karimi

Abstract—**The purpose of this paper is to explore the applicability of linear time-invariant (LTI) dynamical systems with polytopic uncertainty for modeling and control of islanded DC microgrids under plug-and-play (PnP) functionality of distributed generations (DGs). We develop a robust decentralized voltage control framework to ensure robust stability and reliable operation for islanded DC microgrids. The problem of voltage control of islanded DC microgrids with PnP operation of DGs is formulated as a convex optimization problem with structural constraints on some decision variables. The proposed control scheme offers several advantages including decentralized voltage control with no communication link, transient stability/performance, plug-and-play capability, scalability of design, applicability to microgrids with general topology, and robustness to microgrid uncertainties. The effectiveness of the proposed control approach is evaluated through simulation studies carried out in MATLAB/SimPowerSystems Toolbox.**

Index Terms—**Convex optimization, DC microgrids, plug-and-play operation, polytopic uncertainty, robust control, voltage control.**

I. INTRODUCTION

DC microgrids are an efficacious way to integrate renewable energy sources with DC output-type, such as photovoltaics and fuel cells, modern electronic loads, and energy storage systems [1]. These systems propose several advantages: 1) increasing system efficiency due to less conversion losses from sources to loads, 2) no need for the control of frequency, reactive power, and power quality which are known as main challenges in AC microgrids, 3) wide applications in electric vehicles, naval ships, aircrafts, spacecrafts, submarines, and telecom systems [2].

Due to the increasing applicability of DC microgrids and emerging major challenges from the viewpoints of control, new modeling and control techniques must be investigated and explored. A hierarchical control strategy has recently been developed in [3], [4] to standardize the operation and functionality of microgrids. It mainly consists of three control levels with separate time scales named as primary, secondary, and tertiary control. The primary control level, which is typically droop-based, is intended to rapidly stabilize the voltage of DC microgrids and to facilitate an accurate power sharing. The second level with slower time scale compensates for the deviations in the voltage in the steady state induced by the primary control [4]. The tertiary level is associated with optimal operation and power management in DC microrgids [4].

Primary control, which is a proportional controller from a control point of view, has a decentralized structure whereas secondary and tertiary control levels are typically centralized and rely on communication networks [4]. The non-scalability of the centralized control strategies and their non-robustness to single point of failure have promoted a surge of research efforts, e.g. [2], [5]–[19], to partially solve these issues. The solutions are based on distributed control techniques in DC microrgrids where there exist some communication links and information exchange among neighbors.

Another strategy used in islanded microgrids is non-droop-based control, which relies on decentralized advanced model-based control approaches and combines primary and secondary control levels. Non-droop-based control approaches have mostly been used for primary voltage control of AC microgrids [20]–[26]. An example of this control strategy used for DC microrgrids is decentralized scalable state feedback control proposed in [27].

One of the main important issues in microrgrids is plug-and-play (PnP) operation of distributed generations (DGs) due to inherently discontinuous nature of renewable energy sources. The main problem is that PnP functionality of DGs does affect the microgrid stability and deteriorates closed-loop system performance. Although the proposed approach in [27] provides many advantages such as scalability and decentralized structure of primary voltage controllers, it does not allow robust plug-and-play operation. Once a DG is plugged into microgrids or plugged out from the system, the neighbors of that DG have to retune their local primary voltage controllers.

The main objective of this paper is to investigate and develop a new control strategy which provides a solution for the problem of plug-and-play operation in large-scale islanded DC microrgrids. To design such a control strategy, it is necessary to develop an appropriate mathematical model of microgrids that reliably captures the fundamental aspects of the problem. To this end, we consider an islanded DC microgrid with arbitrary topology. Moreover, we assume that the microgrid is subject to a large amount of variability and uncertainty arising from several sources including load variations, microrgid topology change, and plug-and-play operation of DGs. In order to tackle all these issues, we adopt a linear time-invariant (LTI) polytopic system, in which uncertainties are modeled via a convex hull of a set of known vertices. This new representation of DC microgrids enables us to use robust control theory for stability analysis and control of DC microgrids. We develop a robust control strategy for voltage control of islanded DC microrgids. The proposed control strategy offers the following main features: 1) the voltage

M. S. Sadabadi is with the Computational and Biological Learning (CBL) Group, Department of Engineering, University of Cambridge, Cambridge, United Kingdom. Email: mss69@cam.ac.uk

Q. Shafiee is with the Department of Electrical and Computer Engineering, University of Kurdistan, Sanandaj, Kurdistan, Iran. Email: q.shafiee@uok.ac.ir

A. Karimi is with the Automatic Control Laboratory at Ecole Polytechnique Fédérale de Lausanne (EPFL), Lausanne, Switzerland. Email: alireza.karimi@epfl.ch

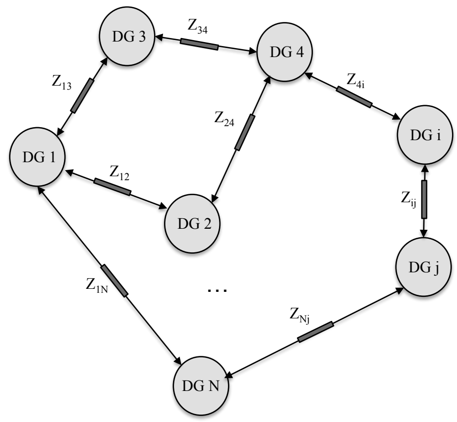

Fig. 1: A schematic diagram of an islanded DC microgrid consisting of N DGs.

controller in primary level is fully decentralized and no digital communication is required, 2) the design procedure is scalable, 3) the controller guarantees stability of the overall microgrid system, 4) the desired transient and steady-state performance of the microrgid system according to IEEE standards [28] are satisfied, 5) it ensures the plug-and-play functionality of DGs, 6) the controller provides robustness with respect to load variations and microgrid topology changes.

The rest of this paper is organized as follows. Section II presents an LTI model with polytopic uncertainty for an islanded DC microgrid under plug-and-play functionality of DGs. Section III is devoted to robust decentralized voltage control of islanded DC microgrids. Simulation case studies are considered in Section IV. Finally, the paper ends with concluding remarks in Section V.

The notation used in this paper is standard. In particular, matrices I and 0 are the identity matrix and the zero matrix of appropriate dimensions, respectively. The symbols A^T and $\star$ denote the transpose of matrix A and symmetric blocks in block matrices, respectively. For symmetric matrices, $P > 0$ and $P < 0$ respectively indicate the positive-definiteness and the negative-definiteness.

II. Mathematical Model of Islanded DC Microgrids

This section is dedicated to the development of an analytical model of an islanded DC microgrid composed of N distributed generations (Fig. 1). In this figure, DG i and DG j are connected via a distribution line Z_{ij} modeled by an RL network with parameters R_{ij} and L_{ij}. A DC microgrid normally consists of DGs and energy storage systems, supplying sort of electronic loads through a common DC bus. The common bus is linked to the distributed energy sources through a DC-DC converter.

Fig. 2a shows a general configuration of DG i connected to DG j via the distribution line interfaced via a DC-DC converter. Depending on the applications, different types of DC-DC converters, e.g. buck and boost are used in DC microgrid systems. Each DG is modeled by a DC voltage source, a DC-DC converter, and a local load whose structure is assumed to be unknown. Signals V_i, V_j, I_{L_i}, and I_{ij} are the load

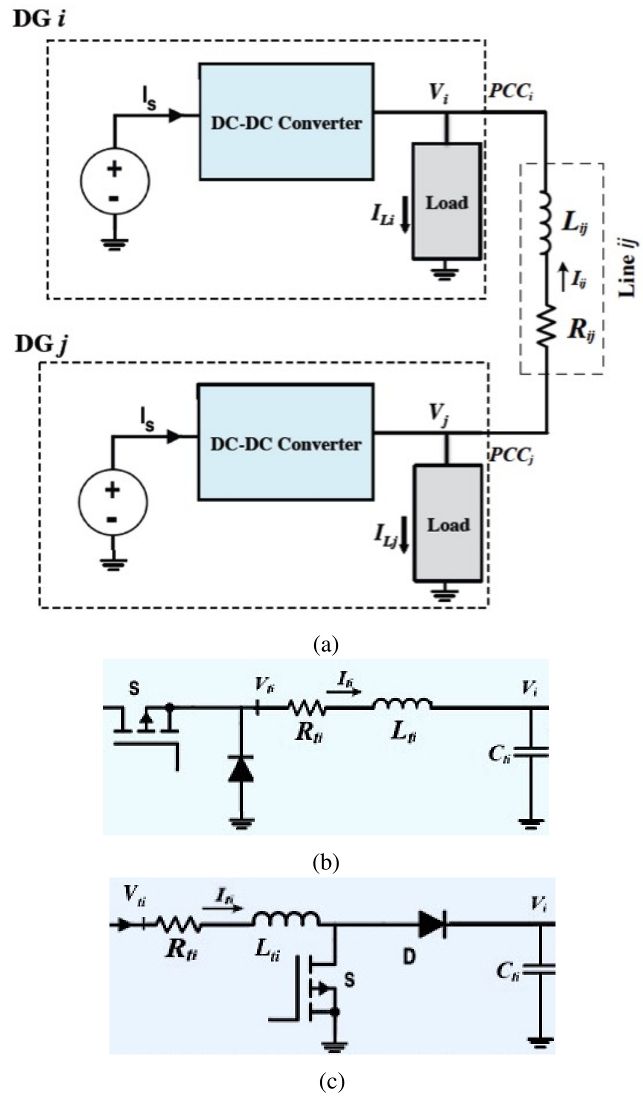

Fig. 2: (a) A General configuration of DG i connected to DG j via distribution line ij and interfaced via a DC-DC converter, (b) A model of a buck converter, and (c) A model of boost converter.

voltage at Point of Common Coupling (PCC i), the voltage at PCC j, the load current, and the distribution line current, respectively.

In what follows, we assume that buck converters are used as DC-DC converters. However, in the case that different DC-DC converters are employed in the DC microrgids, the model of the converter should be considered.

According to Fig. 2b, a buck converter consists of a switching transistor, a series RL filter with parameters R_{t_i} and L_{t_i}, and a shunt capacitor C_{t_i}. Signals I_{t_i} and V_{t_i} are the filter current and the terminal voltage behind RL filter, respectively.

By using the model of a buck converter in [29], the DG i and the distribution line ij are mathematically described by the following dynamical equations:

$$\text{DG } i \begin{cases} \dfrac{dV_i}{dt} = \dfrac{1}{C_{t_i}} I_{t_i} - \dfrac{1}{C_{t_i}} I_{L_i} + \dfrac{1}{C_{t_i}} I_{ij} \\ \dfrac{dI_{t_i}}{dt} = -\dfrac{1}{L_{t_i}} V_i - \dfrac{R_{t_i}}{L_{t_i}} I_{t_i} + \dfrac{d_{buck_i}}{L_{t_i}} V_{t_i} \end{cases} \tag{1}$$

$$\text{Line } ij\text{:}\quad \frac{dI_{ij}}{dt} = -\frac{R_{ij}}{L_{ij}}I_{ij} + \frac{1}{L_{ij}}V_j - \frac{1}{L_{ij}}V_i \tag{2}$$

where d_{buck_i} is the duty cycle of the buck converter i.

A. Quasi Stationary Model of DC Microgrids

It is assumed that the distribution lines have quasi-stationary dynamics, i.e. $\frac{dI_{ij}}{dt} = 0$ [30]. Therefore, the line dynamics in (2) is written as follows:

$$I_{ij} = \frac{V_j - V_i}{R_{ij}} \tag{3}$$

This assumption is reasonable because the line impedance in DC systems is mainly resistive and therefore the inductance L_{ij} can be neglected. By replacing I_{ij} in (1) with (3), the dynamics of DG i are given by:

$$\text{DG } i \begin{cases} \frac{dV_i}{dt} = \frac{1}{C_{t_i}}I_{t_i} - \frac{1}{C_{t_i}}I_{L_i} + \frac{1}{C_{t_i}R_{ij}}V_j - \frac{1}{C_{t_i}R_{ij}}V_i \\ \frac{dI_{t_i}}{dt} = -\frac{1}{L_{t_i}}V_i - \frac{R_{t_i}}{L_{t_i}}I_{t_i} + \frac{d_{buck_i}}{L_{t_i}}V_{t_i} \end{cases} \tag{4}$$

In the same manner, we can show that islanded DC microgrid composed of N DGs in Fig. 1 is described by the following state space equations:

$$\begin{aligned} \dot{x}_{g_i} &= A_{g_{ii}}x_{g_i} + \sum_{j\in N_i} A_{g_{ij}}x_{g_j} + B_{g_i}u_i + B_{w_i}w_i \\ y_i &= C_{g_i}x_{g_i}; \quad i = 1,\ldots,N \end{aligned} \tag{5}$$

where $x_{g_i} = \begin{bmatrix} V_i & I_{t_i} \end{bmatrix}^T$ is the state, $u_i = d_{buck_i}V_{t_i}$ is the input, $w_i = I_{L_i}$ is the exogenous input, and $y_i = V_i$ is the output of DG i. It is assumed that DG i is connected to a set of $N_i \subset \{1,\ldots,N\}$ DGs. The state space matrices are given as follows:

$$\begin{aligned} A_{g_{ii}} &= \begin{bmatrix} -\sum\limits_{j\in N_i} \frac{1}{C_{t_i}R_{ij}} & \frac{1}{C_{t_i}} \\ -\frac{1}{L_{t_i}} & -\frac{R_{t_i}}{L_{t_i}} \end{bmatrix}, \quad A_{g_{ij}} = \begin{bmatrix} \frac{1}{R_{ij}C_{t_i}} & 0 \\ 0 & 0 \end{bmatrix} \\ B_{g_i} &= \begin{bmatrix} 0 \\ \frac{1}{L_{t_i}} \end{bmatrix}, \quad B_{w_i} = \begin{bmatrix} -\frac{1}{C_{t_i}} \\ 0 \end{bmatrix}, \quad C_{g_i} = \begin{bmatrix} 1 & 0 \end{bmatrix} \end{aligned} \tag{6}$$

In equations (5) and (6), the subscript i describes the variables of DG i whereas the subscript j is related to variables of other DGs connected to DG i. More specifically, $(A_{g_{ii}}, B_{g_i}, B_{w_i}, C_{g_i})$ is defined as the state space matrices of DG i. The term $\sum_{j\in N_i} A_{g_{ij}}x_{g_j}$ describes the interaction term between DG i and its connections.

B. Islanded DC Microgrids with Polytopic-type Uncertainty

One of the main sources of uncertainty in microgrids is plug-and-play functionality of DGs. DGs are frequently plugged in and/or plugged out from the microgrid system. As a results, the topology of microgrid is uncertain. In this subsection, we model the PnP operation of DGs in the islanded microgrids as polytopic uncertainty. By virtue of the fact that the plug in/out of DG j to/from DG i affects only the first element of matrix $A_{g_{ii}}$, i.e. $-\frac{1}{C_{t_i}}\sum\limits_{j\in N_i}\frac{1}{R_{ij}}$, we should consider the maximum and minimum values of the term $-\sum\limits_{j\in N_i}\frac{1}{C_{t_i}R_{ij}}$. The minimum value happens when there is maximum possible connections of DGs to DG i. Moreover, the maximum value is associated with a connection with maximum value of R_{ij} among the other N_i connections. Therefore, two cases for each DG are considered:

- Maximum possible connections of DGs to DG i ($N_{i_{max}} \subset \{1,\ldots,N\}$) corresponding to the following vertex:

$$A^1_{g_{ii}} = \begin{bmatrix} -\frac{1}{C_{t_i}}\sum\limits_{j\in N_{i_{max}}}\frac{1}{R_{ij}} & \frac{1}{C_{t_i}} \\ -\frac{1}{L_{t_i}} & -\frac{R_{t_i}}{L_{t_i}} \end{bmatrix} \tag{7}$$

- Connection ij with maximum value of R_{ij} among the other N_i connections which corresponds to the following second vertex:

$$A^2_{g_{ii}} = \begin{bmatrix} -\frac{1}{C_{t_i}}\min_{j\in N_{imax}}\frac{1}{R_{ij}} & \frac{1}{C_{t_i}} \\ -\frac{1}{L_{t_i}} & -\frac{R_{t_i}}{L_{t_i}} \end{bmatrix} \tag{8}$$

If these two vertices are considered as two points, every possible connection/disconnection of DGs to DG i lies in the straight line segment which connects those two points. The line segment connecting two points could mathematically be described as follows:

$$A_{g_{ii}}(\lambda) = \lambda A^1_{g_{ii}} + (1-\lambda)A^2_{g_{ii}} \tag{9}$$

where $0 \leq \lambda \leq 1$. The above uncertainty zone is convex combination of vertices $A^1_{g_{ii}}$ and $A^2_{g_{ii}}$. In other words, the PnP operation of DGs is modeled as a polytopic system.

III. Hierarchical Control of DC Microgrids

The islanded DC microgrid control system proposed in this paper is a hierarchical control strategy which mainly consists of two main levels with separate time-scales. The primary level is intended to stabilize the voltage of the DC microgrids and compensates for the deviations in the voltage in the steady-state. The second level is power management system (PMS) which is associated with the optimal operation of islanded microgrids. Power management system centrally solves an optimal power flow problem and broadcasts respective voltage setpoints to the primary level. This section focuses on the development of a voltage control strategy for autonomous DC microgrids with different types of topologies.

A. Primary Voltage Control

This subsection addresses the voltage controller design of islanded DC microgrids in Fig. 1 with general architecture. We utilize the QSL-based model of the islanded DC microgrid system affected by polytopic uncertainty developed in Section II to design a robust voltage controller. We use IEEE standards [28] to define stability and performance specifications on the control scheme. The proposed control strategy must satisfy the following specifications:

1) The closed-loop system asymptotically tracks all the reference voltage signals and provides the desired transient and steady-state performance according to the IEEE standards [28].
2) The controller guarantees stability of the overall microgrid system.
3) It allows PnP functionality of DGs in microgrids.

4) The controller is robust with respect to load variations and microgrid topology change.
5) The structure of the primary voltage controller is fully decentralized providing several advantages in terms of reliability and cost effectiveness (since each DG is equipped with a local controller with no communication link).

1) Voltage Tracking: To satisfy the aforementioned criterion for the tracking of constant references V_{ref_i}, each DG is augmented with an integrator with the following dynamics:

$$\begin{aligned}\dot{v}_i &= V_{ref_i} - y_i \\ &= V_{ref_i} - C_{g_i} x_{g_i}\end{aligned} \tag{10}$$

Therefore, the augmented model of DG i is described by following state space equations:

$$\begin{aligned}\dot{\hat{x}}_{g_i} &= \hat{A}_{g_{ii}}(\lambda)\hat{x}_{g_i} + \sum_{j\in N_i} \hat{A}_{g_{ij}}\hat{x}_{g_j} + \hat{B}_{g_i}u_i + \hat{B}_{w_i}\hat{w}_i \\ \hat{y}_i &= \hat{C}_{g_i}\hat{x}_{g_i}\end{aligned} \tag{11}$$

where $\hat{x}_{g_i} = \begin{bmatrix} x_{g_i} & v_i \end{bmatrix}^T$, $\hat{y}_i = \begin{bmatrix} y_i & v_i \end{bmatrix}^T$, $\hat{w}_i = \begin{bmatrix} w_i & V_{ref_i} \end{bmatrix}^T$, and

$$\hat{A}_{g_{ii}}(\lambda) = \begin{bmatrix} A_{g_{ii}}(\lambda) & 0 \\ -C_{g_i} & 0 \end{bmatrix}, \quad \hat{A}_{g_{ij}} = \begin{bmatrix} A_{g_{ij}} & 0 \\ 0 & 0 \end{bmatrix}$$
$$\hat{B}_{g_i} = \begin{bmatrix} B_{g_i} \\ 0 \end{bmatrix}, \quad \hat{B}_{w_i} = \begin{bmatrix} B_{w_i} & 0 \\ 0 & I \end{bmatrix}, \quad \hat{C}_{g_i} = \begin{bmatrix} C_{g_i} & 0 \\ 0 & I \end{bmatrix} \tag{12}$$

The augmented matrices $\hat{A}_{g_{ii}}$ are also affected by the polytopic uncertainty:

$$\hat{A}_{g_{ii}}(\lambda) = \lambda\hat{A}^1_{g_{ii}} + (1-\lambda)\hat{A}^2_{g_{ii}} \tag{13}$$

where

$$\hat{A}^1_{g_{ii}} = \begin{bmatrix} A^1_{g_{ii}} & 0 \\ -C_{g_i} & 0 \end{bmatrix}, \quad \hat{A}^2_{g_{ii}} = \begin{bmatrix} A^2_{g_{ii}} & 0 \\ -C_{g_i} & 0 \end{bmatrix} \tag{14}$$

for $i = 1,\dots,N$.

2) Decentralized Robust Voltage Control Scheme: This part is about the design of decentralized robust state feedback controllers K_i with the following control laws:

$$u_i(t) = K_i\hat{x}_{g_i}(t); \quad i = 1,2,\dots,N \tag{15}$$

The closed-loop system of the i^{th} augmented subsystem with polytopic uncertainty in (13)-(14) and its local controller K_i is described as follows:

$$\begin{aligned}\dot{\hat{x}}_{g_i}(t) &= (\hat{A}_{g_{ii}}(\lambda) + \hat{B}_{g_i}K_i)\hat{x}_{g_i}(t) + \sum_{j\in N_i}\hat{A}_{g_{ij}}\hat{x}_{g_j}(t) + \hat{B}_{w_i}\hat{w}_i(t) \\ \hat{y}_i(t) &= \hat{C}_{g_i}\hat{x}_{g_i}(t)\end{aligned} \tag{16}$$

The overall closed-loop system is then presented as follows:

$$\begin{aligned}\dot{\hat{x}}(t) &= (\hat{A}(\lambda) + \hat{B}K)\hat{x} + \hat{B}_w\hat{w}(t) \\ \hat{y}(t) &= \hat{C}\hat{x}(t)\end{aligned} \tag{17}$$

where $\hat{x} = [\hat{x}^T_{g_1}\dots\hat{x}^T_{g_N}]^T$, $\hat{w} = [\hat{w}^T_1\dots\hat{w}^T_N]^T$, $\hat{y} = [\hat{y}^T_1\dots\hat{y}^T_N]^T$, and

$$\begin{aligned}\hat{A}(\lambda) &= \begin{bmatrix} \hat{A}_{g_{11}}(\lambda) & \hat{A}_{g_{12}} & \cdots & \hat{A}_{g_{1N}} \\ \hat{A}_{g_{21}} & \hat{A}_{g_{22}}(\lambda) & \cdots & \hat{A}_{g_{2N}} \\ \vdots & \vdots & \ddots & \vdots \\ \hat{A}_{g_{N1}} & \hat{A}_{g_{N2}} & \cdots & \hat{A}_{g_{NN}}(\lambda) \end{bmatrix} \\ \hat{B} &= diag\left(\hat{B}_{g_1},\dots,\hat{B}_{g_N}\right), \quad \hat{B}_w = diag\left(\hat{B}_{w_1},\dots,\hat{B}_{w_N}\right) \\ \hat{C} &= diag\left(\hat{C}_{g_1},\dots,\hat{C}_{g_N}\right), \quad K = diag\left(K_1,\dots,K_N\right)\end{aligned} \tag{18}$$

The decentralized robust state feedback controller is designed via the following theorem which is based on the use of two slack variables Y and G [31].

Theorem 1. *The decentralized state feedback K stabilizes the closed-loop system with polytopic uncertainty in (17) if there exist positive-definite matrices $P^l = diag\left(P^l_1,\dots,P^l_N\right)$, diagonal slack matrices $G = diag\left(G_1,\dots,G_N\right)$ and $Y = diag\left(Y_1,\dots,Y_N\right)$, and a scalar $\varepsilon > 0$ such that the following conditions hold:*

$$\begin{bmatrix} \hat{A}^lG + G^T(\hat{A}^l)^T + \hat{B}Y + Y^T\hat{B}^T & \star \\ P^l - G + \varepsilon(G^T(\hat{A}^l)^T + Y^T\hat{B}^T) & -\varepsilon(G+G^T) \end{bmatrix} < 0 \tag{19}$$

where

$$\hat{A}^l = \begin{bmatrix} \hat{A}^l_{g_{11}} & \hat{A}_{g_{12}} & \cdots & \hat{A}_{g_{1N}} \\ \hat{A}_{g_{21}} & \hat{A}^l_{g_{22}} & \cdots & \hat{A}_{g_{2N}} \\ \vdots & \vdots & \ddots & \vdots \\ \hat{A}_{g_{N1}} & \hat{A}_{g_{N2}} & \cdots & \hat{A}^l_{g_{NN}} \end{bmatrix} \tag{20}$$

for $l = 1,2$. Moreover, the robust state feedback controllers are presented as $K_i = Y_iG_i^{-1}$ and stabilize the system $(\hat{A}_{g_{ii}}(\lambda),\hat{B}_{g_i},\hat{C}_{g_i},0)$ with a linearly parameter dependent Lyapunov matrix $P_i(\lambda) = \lambda P^1_i + (1-\lambda)P^2_i$, where $0 \le \lambda \le 1$.

Theorem 1 proposes some Linear Matrix Inequalities (LMIs) for design of a robust decentralized state feedback controller. It is based on the use of slack matrices (G,Y). If the LMI conditions in (19) are held, the closed-system with the robust decentralized state feedback controller can satisfy the stability condition according to Lyapunov theory [31]. By solving the set of LMIs in (19), the robust state feedback controller for each DG is obtained as $K_i = Y_iG_i^{-1}$, $i = 1,...,N$.

Remark. Theorem 1 is about the design of robust state-feedback controllers for uncertain systems where the uncertainty is modeled in terms of polytopic matrices $A_{g_{ii}}(\lambda)$ and $\hat{A}_{g_{ii}}(\lambda)$. If LMI conditions in (19) are satisfied for $l = 1,2$, i.e.

$$\begin{bmatrix} \hat{A}^lG + G^T(\hat{A}^l)^T + \hat{B}Y + Y^T\hat{B}^T & \star \\ P^l - G + \varepsilon(G^T(\hat{A}^l)^T + Y^T\hat{B}^T) & -\varepsilon(G+G^T) \end{bmatrix} < 0 \tag{21}$$

Then, the following inequality obtained by convex combination of above inequalities is also held:

$$\begin{bmatrix} \hat{A}(\lambda)G + G^T\hat{A}^T(\lambda) + \hat{B}Y + Y^T\hat{B}^T & \star \\ P(\lambda) - G + \varepsilon(G^T\hat{A}^T(\lambda) + Y^T\hat{B}^T) & -\varepsilon(G+G^T) \end{bmatrix} < 0 \tag{22}$$

where $\hat{A}(\lambda) = \lambda\hat{A}^1 + (1-\lambda)\hat{A}^2$ and $P(\lambda) = \lambda P^1 + (1-\lambda)P^2$. The above condition proves the stability of the system affected by uncertainty (robustness to uncertainty).

To design the local voltage controllers K_i using Theorem 1, the coupling terms $\sum_{j\in N_i}\hat{A}_{g_{ij}}\hat{x}_{g_j}$ are considered. However, we aim to design the local controllers K_i individually without considering the interactions among different DGs such that the asymptotic stability of the closed-loop DC microgrid system is guaranteed.

In the following, we show that under some specific conditions mainly on the slack matrices G_i, the interaction terms in the augmented microgrid model described by (17)-(18) are neutral, i.e. they do not affect the closed-loop stability. As a result, the decentralized design of the local voltage controllers guarantees the stability of the whole microgrid system, i.e. $\hat{A}(\lambda)$.

If the following conditions are met, the interaction terms in the augmented microgrid model described by (17)-(18) are neutral.

1) Slack matrices G_i have the following structure:

$$G_i = \left[\begin{array}{c|c} \eta_i & [0 \quad 0] \\ \hline G_{21_i} & G_{22_i} \end{array} \right]; \quad i = 1, \ldots, N \tag{23}$$

where $\eta_i > 0$ and matrices G_{21_i} and G_{22_i} are of appropriate dimensions.

2) $\frac{\eta_i}{R_{ij} C_{t_i}} \approx 0$ for $i = 1, \ldots, N$ and $j \in N_i$.

If the above mentioned conditions hold, the interaction terms $\hat{A}^l_{g_{ji}} G_j + G_j^T (\hat{A}^l_{g_{ij}})^T \approx 0$ for $l = 1, 2$ because

$$\begin{aligned} \hat{A}^l_{g_{ij}} G_j = G_j^T (\hat{A}^l_{g_{ij}})^T &= \begin{bmatrix} \frac{\eta_i}{R_{ij} C_{t_i}} & 0 & 0 \\ 0 & 0 & 0 \\ 0 & 0 & 0 \end{bmatrix} \\ &\approx \begin{bmatrix} 0 & 0 & 0 \\ 0 & 0 & 0 \\ 0 & 0 & 0 \end{bmatrix} \end{aligned} \tag{24}$$

The first condition can be satisfied by considering the structural constraint given in (23) on the slack matrices G_i in the LMI conditions in (19). The second condition is also met if $\eta_i > 0$ is minimized or considered to have a very small value.

B. Pre-filter Design

The local controllers K_i designed in the previous subsection are stabilizing controllers. However, to improve the performance of the closed-loop system in terms of dynamics behaviour for voltage reference tracking according to IEEE standards [28], a feedforward controller K_i^r is developed. The closed-loop system including the stabilizing and feedforward controllers is described as follows:

$$y_i = (T_i(s) K_i^r(s)) V_{ref_i} \tag{25}$$

where

$$T_i(s) = \hat{C}_i \left(sI - (\hat{A}_{g_{ii}} + \hat{B}_{g_i} K_i) \right)^{-1} \begin{bmatrix} 0 \\ I \end{bmatrix} \tag{26}$$

To achieve desired time-domain performance specifications for reference tracking, the feedforward controllers $K_i^r(s)$ are designed by solving the following H_∞ optimization problem:

$$\begin{aligned} &\min_{K_i^r} \quad \gamma_i \\ &\text{s.t.} \quad \| T_i(s) K_i^r(s) - T_{d_i}(s) \|_\infty < \gamma_i \end{aligned} \tag{27}$$

where $T_{d_i}(s)$ is a desired reference tracking (reference model) designed according to the desired performance of DG i.

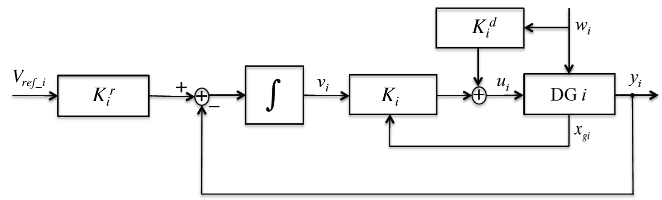

Fig. 3: Block diagram of overall control system of DG i.

C. Robustness to Load Changes

In the DC microrgid in Fig. 2a, the topology of load is unknown and load is assumed to be structurally uncertain. However, it is assume that the load current I_L is available and measurable. We consider the load current as a measurable disturbance signal. To effectively attenuate the effects from the disturbance signal on the output signal, a feedforward controller K_i^d is designed. The closed-loop transfer function from the disturbance signal I_{L_i} to the output signal y_i is as follows:

$$y_i = \left(H_i(s) K_i^d(s) + H_i^d(s) \right) I_{L_i} \tag{28}$$

where

$$\begin{aligned} H_i(s) &= \hat{C}_i \left(sI - (\hat{A}_{g_{ii}} + \hat{B}_{g_i} K_i) \right)^{-1} \hat{B}_{g_i} \\ H_i^d(s) &= \hat{C}_i \left(sI - (\hat{A}_{g_{ii}} + \hat{B}_{g_i} K_i) \right)^{-1} \hat{B}_{w_i} \end{aligned} \tag{29}$$

Then, the minimization of the impact of load changes on the voltages at PCCs can be achieved by means of solving the following optimization problem:

$$\begin{aligned} &\min_{K_i^d} \quad \beta_i \\ &\text{s.t.} \quad \| H_i(s) K_i^d(s) + H_i^d(s) \|_\infty < \beta_i \end{aligned} \tag{30}$$

In this optimization problem, the aim is to design a feedforward controller K_i^d such that H_∞ norm of the closed-loop transfer function from the disturbance signal to the output signal described in (28) is minimized. Therefore, in the optimization problem proposed in (30), we would like to minimize the upper bound of the H_∞ norm (cost function) of the transfer function. The unknown variable is the feedforward controller $K_i^d(s)$.

Fig.3 shows a block diagram of the control system of each DG in the DC microgrid system.

Remark. The optimization problems in (27) and (30) can be solved using some developed control approaches in the literature, e.g. [32], [33].

D. Algorithm for Decentralized Voltage Control of Islanded DC Microgrids

In this subsection, a systematic algorithm for the design of the local voltage controllers K_i and the supplementary controllers K_i^r and K_i^d for the DG i described by (17)-(18) is given. The algorithm includes the following steps:

Step 1: Vertices of polytope. Build two vertices $A^1_{g_{ii}}$ and $A^2_{g_{ii}}$ respectively given in (7) and (8) as well as augmented matrices $\hat{A}^1_{g_{ii}}$ and $\hat{A}^2_{g_{ii}}$ in (14) for $i = 1, \ldots, N$.

Step 2: Fixed-structure slack matrices. Fix the structure of the slack matrices G_i as follows:

$$G_i = \left[\begin{array}{c|c} \eta_i & [0 \quad 0] \\ \hline G_{21_i} & G_{22_i} \end{array}\right]; \quad i = 1,\ldots,N \tag{31}$$

where G_{21_i} and G_{22_i} are considered as decision variables in optimization problem.

Step 3: Convex optimization problem. Fix the scalar parameter $\varepsilon_i > 0$ and solve the following convex optimization problem to obtain the voltage controllers K_i:

$$\begin{aligned} &\min_{Y_i, P_i^l, G_{21_i}, G_{22_i}} \quad \eta_i \\ &\text{s.t.} \begin{bmatrix} \hat{A}_{g_{ii}}^l G_i + G_i^T(\hat{A}_{g_{ii}}^l)^T + \hat{B}_{g_i} Y_i + Y_i^T \hat{B}_{g_i}^T & \star \\ P_i^l - G_i + \varepsilon_i(\hat{A}_{g_{ii}}^l G_i + \hat{B}_{g_i} Y_i)^T & -\varepsilon_i(G_i + G_i^T) \end{bmatrix} < 0 \\ &\qquad P_i^l > 0 \\ &\qquad\quad i = 1,\ldots,N; \quad l = 1,2 \end{aligned} \tag{32}$$

Remark. The optimization in (32) is about the design of robust state feedback controller for DG i under neutral interaction. Therefore, we have to consider the conditions (1) and (2) proposed in Section III-A-2. According to condition (2), $\frac{\eta_i}{R_{ij}C_{t_i}} \approx 0$ for $i = 1,\ldots,N$ and $j \in N_i$. Therefore, we would like to minimize η_i (cost function) subject to the stability condition in (19) (constraints).

Step 4: Stabilizing voltage controllers. The robust local voltage controllers are presented as $K_i = Y_i G_i^{-1}$, $i = 1,\ldots,N$.

Step 5: Pre-filter design. Design pre-filters for controller performance improvement and disturbance rejection.

E. Robustness to Constant Power Loads

Constant Power Loads (CPLs) provide challenging issues from the stability point of view as they introduce negative impedances seen from the main bus [34]. In this subsection, we analyze the stability of DG i under the proposed voltage control technique against CPLs. To this end, it is assumed that DG i supplies a CPL with power demand P_{CPL} connected at PCC i.

The state space equations which describe the dynamics of DG i are as follows:

$$\frac{d}{dt}\begin{bmatrix} V_i \\ I_{t_i} \end{bmatrix} = \begin{bmatrix} -\frac{1}{C_{t_i}}\sum_{j\in N_i}\frac{1}{R_{ij}} & \frac{1}{C_{t_i}} \\ -\frac{1}{L_{t_i}} & -\frac{R_{t_i}}{L_{t_i}} \end{bmatrix}\begin{bmatrix} V_i \\ I_{t_i} \end{bmatrix} + \sum_{j\in N_i}\begin{bmatrix} \frac{1}{R_{ij}C_{t_i}} & 0 \\ 0 & 0 \end{bmatrix}\begin{bmatrix} V_j \\ I_{t_j} \end{bmatrix} + \begin{bmatrix} 0 \\ \frac{1}{L_{t_i}} \end{bmatrix} d_{buck_i} V_{t_i} + \begin{bmatrix} -\frac{1}{C_{t_i}} \\ 0 \end{bmatrix}\frac{P_{CPL}}{V_i} \tag{33}$$

The above equation is nonlinear with respect to V_i due to the nonlinear term $\frac{P_{CPL}}{V_i}$. Linearization of (33) around operating points leads to the following model:

$$\frac{d}{dt}\begin{bmatrix} V_i - V_{i_0} \\ I_{t_i} - I_{t_{i0}} \end{bmatrix} \approx \begin{bmatrix} -\frac{1}{C_{t_i}}\left(\sum_{j\in N_i}\frac{1}{R_{ij}} - \frac{P_{CPL}}{V_{i_0}^2}\right) & \frac{1}{C_{t_i}} \\ -\frac{1}{L_{t_i}} & -\frac{R_{t_i}}{L_{t_i}} \end{bmatrix}\begin{bmatrix} V_i - V_{i_0} \\ I_{t_i} - I_{t_{i0}} \end{bmatrix} + \sum_{j\in N_i}\begin{bmatrix} \frac{1}{R_{ij}C_{t_i}} & 0 \\ 0 & 0 \end{bmatrix}\begin{bmatrix} V_j - V_{j_0} \\ I_{t_j} - I_{t_{j0}} \end{bmatrix} + \begin{bmatrix} 0 \\ \frac{1}{L_{t_i}} \end{bmatrix}(\hat{V}_{t_i} - \hat{V}_{t_{i0}}) \tag{34}$$

where $\hat{V}_{t_i} = d_{buck_i} V_{t_i}$ and $(V_{i_0}, V_{j_0}, I_{t_{i0}}, V_{t_{i0}})$ are the operating points of the DC microgrid system. The state feedback control rule is $\hat{V}_{t_i} - \hat{V}_{t_{i0}} = K_i \begin{bmatrix} V_i - V_{i_0} \\ I_{t_i} - I_{t_{i0}} \end{bmatrix}$, where $K_i = \begin{bmatrix} k_{i_1} & k_{i_2} \end{bmatrix}$. Therefore, the closed-loop state matrix is as follows:

$$A_{cl_i} = \begin{bmatrix} -\frac{1}{C_{t_i}}\left(\sum_{j\in N_i}\frac{1}{R_{ij}} - \frac{P_{CPL}}{V_{i_0}^2}\right) & \frac{1}{C_{t_i}} \\ \frac{-1+k_{i_1}}{L_{t_i}} & \frac{-R_{t_i}+k_{i_2}}{L_{t_i}} \end{bmatrix} \tag{35}$$

Necessary and sufficient conditions for the stability of the closed-loop system are $trace(A_{cl_i}) < 0$ and $det(A_{cl_i}) > 0$. In other words, the control parameters must satisfy the following conditions in order to preserve the stability of the DC microgrid system under CPLs:

$$\begin{aligned} k_{i_1} &< \left(\sum_{j\in N_i}\frac{1}{R_{ij}} - \frac{P_{CPL}}{V_{i_0}^2}\right)(R_{t_i} - k_{i_2}) + 1 \\ k_{i_2} &< \frac{L_{t_i}}{C_{t_i}}\left(\sum_{j\in N_i}\frac{1}{R_{ij}} - \frac{P_{CPL}}{V_{i_0}^2}\right) + R_{t_i} \end{aligned} \tag{36}$$

By adding the above constraints on the controller parameters to the optimization problem in (32), the designed controller is robust to CPLs.

F. Voltage Control of DC Microgrids with Boost Converters

In this subsection, it is assumed that boost converters with the general model shown in Fig. 2c are used in the DC microgrid system in Fig. 2a. In this case, the DG i with N_i connections to its neighbors is mathematically described as follows:

$$\text{DG } i \begin{cases} \frac{dV_i}{dt} = \frac{(1-d_{boost_i})}{C_{t_i}} I_{t_i} - \frac{1}{C_{t_i}} I_{L_i} + \frac{1}{C_{t_i}} \sum_{j\in N_i} \frac{V_j - V_i}{R_{ij}} \\ \frac{dI_{t_i}}{dt} = -\frac{(1-d_{boost_i})}{L_{t_i}} V_i - \frac{R_{t_i}}{L_{t_i}} I_{t_i} + \frac{1}{L_{t_i}} V_{t_i} \end{cases} \tag{37}$$

where d_{boost_i} is the duty cycle of the boost converter i.

In this current framework, the control signal is the duty cycle d_{boost_i}. However, due to two bilinear terms $(1 - d_{boost_i})I_{t_i}$ and $(1 - d_{boost_i})V_{t_i}$ in (37), the system is not linear. The following model is resulted from the linearization of equation (37) around fixed points $(V_{i_0}, V_{j_0}, I_{t_{i0}}, I_{L_{i0}}, d_{boost_{i_0}})$:

$$\frac{d}{dt}\begin{bmatrix} V_i - V_{i_0} \\ I_{t_i} - I_{t_{i0}} \end{bmatrix} \approx \begin{bmatrix} -\frac{1}{C_{t_i}}\sum_{j\in N_i}\frac{1}{R_{ij}} & \frac{(1-d_{boost_{i_0}})}{C_{t_i}} \\ -\frac{(1-d_{boost_{i_0}})}{L_{t_i}} & -\frac{R_{t_i}}{L_{t_i}} \end{bmatrix}\begin{bmatrix} V_i - V_{i_0} \\ I_{t_i} - I_{t_{i0}} \end{bmatrix} + \sum_{j\in N_i}\begin{bmatrix} \frac{1}{R_{ij}C_{t_i}} & 0 \\ 0 & 0 \end{bmatrix}\begin{bmatrix} V_j - V_{j_0} \\ I_{t_j} - I_{t_{j0}} \end{bmatrix} + \begin{bmatrix} -\frac{1}{C_{t_i}} \\ 0 \end{bmatrix}(I_{L_i} - I_{L_{i0}}) + \begin{bmatrix} \frac{I_{t_{i0}}}{C_{t_i}} \\ -\frac{V_{i_0}}{L_{t_i}} \end{bmatrix}(-d_{boost_i} + d_{boost_{i_0}}) \tag{38}$$

TABLE I: Electrical parameters of microgrid in Fig. 4

DGs	DC-DC converter parameters $R_t(\Omega)$	$L_t(mH)$	Shunt capacitance $C_t(mF)$	Load parameter $R(\Omega)$	Reference voltage V_{ref} (V)
DG 1	0.2	1.8	2.2	10	47.9
DG 2	0.3	2.0	1.9	6	48
DG 3	0.1	2.2	1.7	20	47.7
DG 4	0.5	3.0	2.5	2	48
DG 5	0.4	1.2	2.0	4	47.8
DG 6	0.6	2.5	3.0	8	48.1
DC bus voltage			$V_{dc} = 100$ V		
Switching frequency			$f_{sw} = 10$ kHz		
System nominal frequency			$f_0 = 60$ Hz		

TABLE II: Parameters of distribution network in Fig. 4

Line impedance Z_{ij}	$R_{ij}(\Omega)$	$L_{ij}(\mu H)$
Z_{12}	0.05	2.1
Z_{13}	0.07	1.8
Z_{34}	0.06	1.0
Z_{24}	0.04	2.3
Z_{45}	0.08	1.8
Z_{16}	0.1	2.5
Z_{56}	0.08	3.0

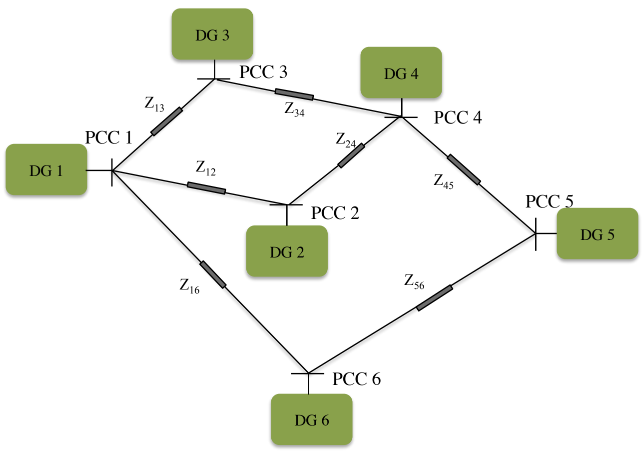

Fig. 4: Layout of an islanded DC microgrid consisting of 6 DGs.

The model is presented in state space framework as equation (5) where $u_i = -d_{boost_i} + d_{boost_{i0}}$ and

$$A_{g_{ii}} = \begin{bmatrix} -\sum\limits_{j\in N_i} \frac{1}{C_{t_i} R_{ij}} & \frac{(1-d_{boost_{i0}})}{C_{t_i}} \\ -\frac{(1-d_{boost_{i0}})}{L_{t_i}} & -\frac{R_{t_i}}{L_{t_i}} \end{bmatrix}, \quad A_{g_{ij}} = \begin{bmatrix} \frac{1}{R_{ij} C_{t_i}} & 0 \\ 0 & 0 \end{bmatrix}$$
$$B_{g_i} = \begin{bmatrix} \frac{I_{i0}}{C_{t_i}} \\ -\frac{V_{i0}}{L_{t_i}} \end{bmatrix}, \quad B_{w_i} = \begin{bmatrix} -\frac{1}{C_{t_i}} \\ 0 \end{bmatrix}, \quad C_{g_i} = \begin{bmatrix} 1 & 0 \end{bmatrix} \tag{39}$$

The proposed voltage control strategy in Section III can be applied to DGs with boost converters modeled as (5) and (39).

IV. Simulation Results

To evaluate the performance of the proposed control scheme, we consider an islanded DC microgrid consisting of 6 DGs with buck converters, taken from [27], as graphically shown in Fig. 4. The parameters of each DG and the distribution network are respectively given in Table I and Table II. To design a robust voltage controller for each DG, it is necessary to develop a polytopic model. Therefore, according to Step

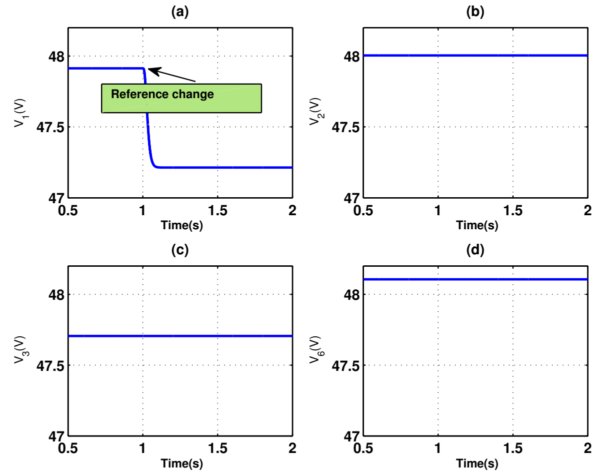

Fig. 5: Dynamic response of DG1 and its neighbors due to reference change at $t = 1$ s: (a) voltage signal at PCC1, (b) voltage signal at PCC 2, (c) voltage signal at PCC 3, and (d) voltage signal at PCC6.

1 of the algorithm proposed in Subsection III-D, all possible connections of DGs are considered. The convex optimization problems in (32) are solved using YALMIP [35] as an interface and MOSEK [36] as a solver. The simulation case studies are carried out in SimPowerSystems Toolbox of MATLAB. It is notable to mention that the inductance L_{ij} of the distribution network is not ignored in the simulation case studies.

Remark: Transient behavior of microrgids is really important and affects the stability and normal operation of microgrids. Some standards about desired transient performance are given in [28]. One of the most important requirements about the controller strategy for microgrids is that the closed-loop DC microgrid system with the controller provides stability, desired transient, and steady-state performance according to the IEEE standards in [28]. Therefore, the main focus of the following case studies is on the transient performance of DGs.

A. Case Study 1: Voltage tracking

The first case study assesses the performance and the transient response of DGs in voltage tracking. The voltage references for all DGs are initially set according to reference values given in Table I. Then, the voltage reference for DG1 is stepped down to 47.2 V at $t = 1$ s. Fig. 5 shows the dynamic responses of DG1 and its neighbors in the DC microgrid system. The results show that the proposed control technique is able to regulate the load voltage at PCCs with zero steady state error and small transient time.

B. Case Study 2: PnP functionality of DGs

In the second case study, we evaluate the capability of the proposed controllers in PnP functionality of DGs. To this end, it is assumed that DG5 is plugged out from the microgrid system in Fig. 4 at $t = 1$ s and it is plugged in at $t = 2$ s. Due to this PnP operation, all the connection attached to DG5, i.e. DG4 and DG6, are affected.

Fig. 6 shows the load voltages of DG5 and its neighbors at PCCs. The results illustrate that the PnP functionality of DG5

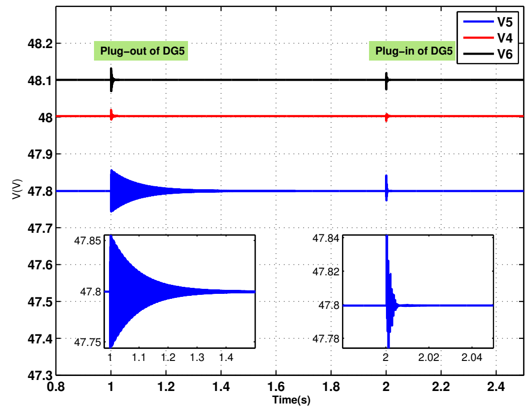

Fig. 6: Dynamic response of DG5 and its neighbors due to plug-out of DG5 at $t = 1$ s and its plug-in at $t = 2$ s.

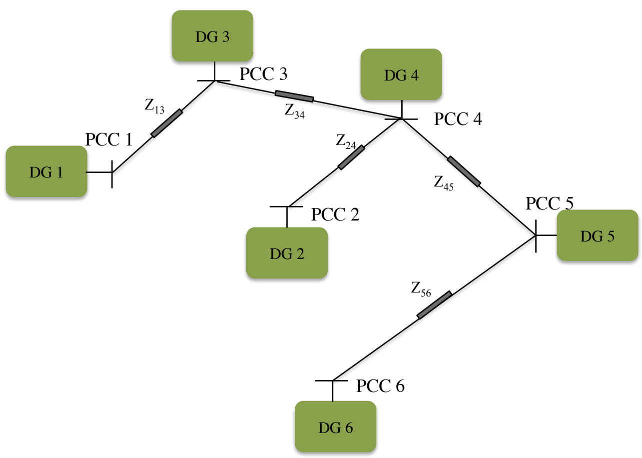

Fig. 7: Layout of islanded DC microgrid consisting of 6 DGs after topology change.

does not influence the stability of the microgrid system. In other words, the DC microgrid system is robustly stable with respect to PnP operation of DGs. Consequently, no redesigning procedure for the local controllers is required.

C. *Case Study 3: Microgrid topology change*

In this case study, we assume that the line between DG1 and DG2 and the line between DG1 and DG6 are respectively disconnected at $t = 1$ s ant $t = 1.3$ s due to faults. As a result, the topology of the DC microrgrid system changes as shown in Fig. 7. The dynamical response of DG1, DG2, and DG6 due to this microrgid topology change is plotted in Fig. 8. The results reveal the robust performance of the voltage controllers to uncertainties affected the microgrid topology.

D. *Case Study 4: Load change*

Case study 4 evaluates the performance of the proposed control strategy in load uncertainty. To this end, the load resistance at PCC6 is stepped down from 8 Ω to 4 Ω at $t = 1$ s. Fig. 9 shows the voltage signals at PCC6, PCC1, and PCC5 as well as the injected power of DG6. The dynamical responses confirm that the voltage controllers are robust with respect to load variations.

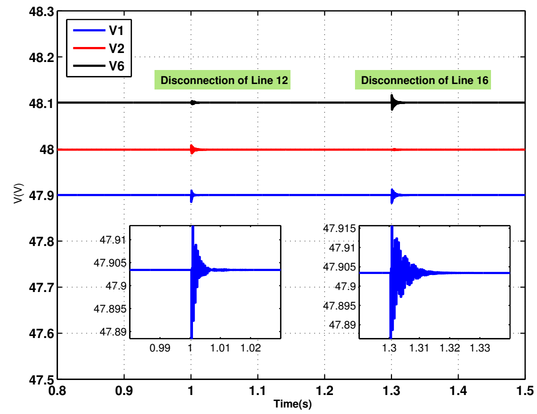

Fig. 8: Dynamic response of DG1, DG2, and DG6 due to changes in microgrid topology at $t = 1$ s and $t = 1.3$ s.

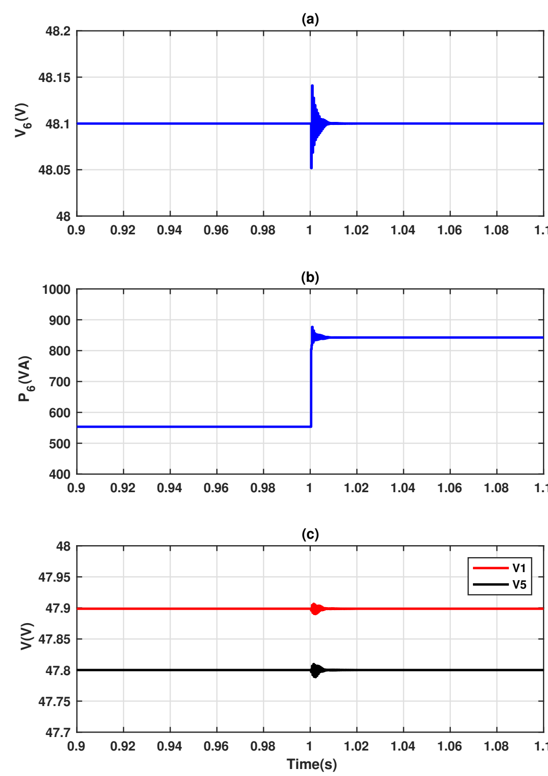

Fig. 9: Dynamic response of DG6 and its neighbors due to a load change at PCC6 at $t = 1$ s. (a) Voltage at PCC6, (b) Injected power of DG6, and (c) Voltage at PCC1 and PCC5.

E. *Case Study 5: Comparison*

The performance of the proposed voltage control approach in terms of PnP operation of DGs is compared with the one in [27]. To this end, it is assumed that DG5 is plugged out at $t = 4$ s and it is then plugged into the microgrid at $t = 6$ s. The results obtained via the control strategy in [27] and proposed control approach are depicted in Fig. 10. Similar to the proposed voltage control design approach, the voltage control strategy in [27] has many advantages including scalability

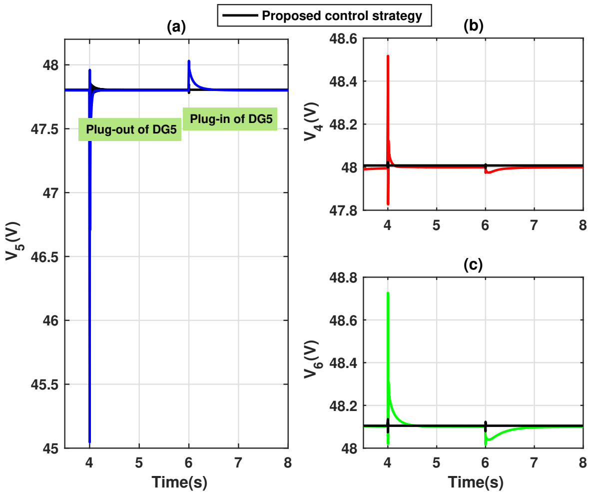

Fig. 10: Performance of voltage control strategy in [27] and proposed control technique during plug-out of DG5 at $t = 4s$ and its plug-in at $t = 6s$. (a) Voltage at PCC 5, (b) Voltage at PCC 4, and (c) Voltage at PCC 6.

and decentralized architecture of primary voltage controllers. However, it does not provide robustness with respect to PnP operation of DGs. In order to make a smooth and fast transient response, the voltage control strategy in [27] needs to retune the local voltage controller of DG5. Comparison between the dynamical responses of both voltage strategies in Fig. 10 in terms of transient behavior shows the superiority of the proposed voltage control strategy in robustness against PnP functionality of DGs.

F. Case Study 6: DC microgrids with different types of DC-DC converters

To show that the proposed voltage control technique is not limited to DC microrgrids with only buck converters, we assume that in the DC microgrid of Fig. 4, realistic boost converters are used in DG1 and DG2 and the other DGs are based on buck topology. New voltage controllers for DG1 and DG2 are designed according to the algorithm proposed in Subsection III-D and the model given in Subsection III-F. The case study 2 is repeated for this new structure of DC microgrid and the results are depicted in Fig. 11.

V. Conclusions

In this paper, we develop a new method for modeling and control of islanded DC microgrids. We adopt an LTI model with polytopic-type uncertainty in order to tackle main sources of uncertainties in microgrids including microgrid topology change and plug-and-play operation of DGs. Then, a decentralized robust voltage controller is designed via an optimal solution of a convex optimization problem. The main advantage of the proposed control approach is its robustness to plug-and-play functionality of DGs and consequently re-designing procedure is not required when DGs are plugged in/out. Moreover, the control strategy does not create any steady state error, thus no secondary controller is required. Various case studies are carried out in MATLAB to evaluate the performance of the proposed control strategy in terms

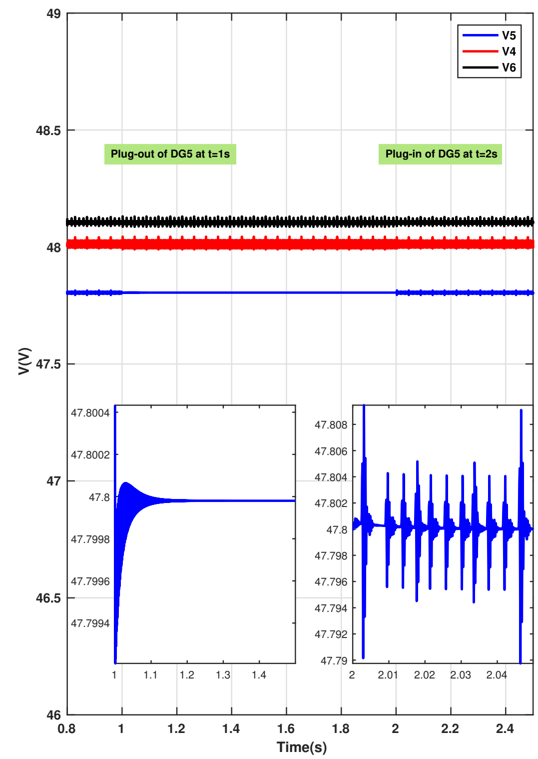

Fig. 11: Performance evaluation of the proposed control strategy under plug-out of DG5 at $t = 1s$ and its plug-in at $t = 2s$ in Case study 6.

of voltage regularization, microgrid topology change, load disturbances, and plug-and-play capability features of DGs.

VI. Acknowledgment

This research work is financially supported by the Swiss National Science Foundation under Grant No. 200020-130528. The authors also acknowledge the CTI- Commission for Technology and Innovation (CH), and the SCCER-FURIES-Swiss Competence Center for Energy Research- Future Swiss Electrical Infrastructure, for their financial and technical support to the research activity presented in this paper.

References

[1] A. T. Elsayed, A. A. Mohamed, and Q. A. Mohammed, "DC microgrids and distribution systems: An overview," *Electric Power Systems Research*, vol. 119, no. 4, pp. 407–417, Feb. 2015.

[2] Q. Shafiee, T. Dragicevic, J. C. Vasquez, and J. M. Guerrero, "Hierarchical control for multiple DC-microgrids clusters," *IEEE Trans. Energy Convers.*, vol. 29, no. 4, pp. 1018–1031, Dec. 2014.

[3] J. M. Guerrero, J. C. Vasquez, J. Matas, L. G. de Vicuna, and M. Castilla, "Hierarchical control of droop-controlled AC and DC microgrids–A general approach towards standardization," *IEEE Trans. Ind. Electron.*, vol. 58, no. 1, pp. 158–172, Jan. 2011.

[4] J. M. Guerrero, M. Chandorkar, T. Lee, and P. C. Loh, "Advanced control architectures for intelligent microgrids–Part I: Decentralized and hierarchical control," *IEEE Trans. Ind. Electron.*, vol. 60, no. 4, pp. 1254–1262, Apr. 2013.

[5] S. Anand, B. G. Fernandes, and M. Guerrero, "Distributed control to ensure proportional load sharing and improve voltage regulation in low-voltage DC microgrids," *IEEE Trans. Power Electron.*, vol. 28, no. 4, pp. 1900–1913, Apr. 2013.

[6] X. Lu, M. Guerrero, K. Sun, and J. C. Vasquez, "An improved droop control method for DC microgrids based on low bandwidth communication with DC bus voltage restoration and enhanced current sharing accuracy," *IEEE Trans. Power Electron.*, vol. 29, no. 4, pp. 1800–1812, Apr. 2014.

[7] L. Meng, T. Dragicevic, J. M. Guerrero, and J. C. Vasquez, "Dynamic consensus algorithm based distributed global efficiency optimization of a droop controlled DC microgrid," in *IEEE Energy Conference (ENERGYCON14)*, Cavtat, Croatia, May 2014, pp. 1276–1283.

[8] Q. Shafiee, T. Dragicevic, F. Andrade, J. C. Vasquez, and J. M. Guerrero, "Distributed consensus-based control of multiple DC-microgrids clusters," in *IECON 2014 - 40th Annu. Conf. IEEE Ind. Electron. Soc.*, Oct.-Nov. 2014, pp. 2056–2062.

[9] V. Nasirian, A. Davoudi, and F. L. Lewis, "Distributed adaptive droop control for DC microgrids," *IEEE Trans. Energy Convers.*, vol. 29, no. 4, pp. 1147–1152, Dec. 2014.

[10] P. Wang, X. Lu, X. Yang, W. Wang, and D. G. Xu, "An improved distributed secondary control method for DC microgrids with enhanced dynamic current sharing performance," *IEEE Trans. Power Electron.*, vol. 31, no. 9, pp. 6658–6673, Sep. 2016.

[11] J. Zhao and F. Dorfler, "Distributed control, load sharing, and dispatch in DC microgrids," in *American Control Conference (ACC)*, Chicago, IL, Jul. 2015, pp. 3304–3309.

[12] T. R. Oliveira, W. W. A. G. Silva, and P. F. Donoso-Garcia, "Distributed secondary level control for energy storage management in DC microgrids," *IEEE Trans. Smart Grid*, 2016. [Online]. Available: http://ieeexplore.ieee.org/stamp/stamp.jsp?arnumber=7423808

[13] P. Wang, J. Xiao, and L. Setyawan, "Hierarchical control of hybrid energy storage system in DC microgrids," *IEEE Trans. Ind. Electron.*, vol. 62, no. 8, pp. 4915–4924, Aug. 2015.

[14] L. Meng, T. Dragicevic, J. Vasquez, J. Guerrero, and E. R. Sanseverino, "Hierarchical control with virtual resistance optimization for efficiency enhancement and state-of-charge balancing in DC microgrids," in *IEEE 1st Int. Conf. Direct Curr. Microgrids (ICDCM)*, Atlanta, Georgia, June 2015.

[15] N. Eghtedarpour and E. Farjah, "Distributed charge/discharge control of energy storages in a renewable-energy-based DC micro-grid," *IET Renew. Power Gener.*, vol. 8, no. 1, pp. 45–57, Jan. 2014.

[16] V. Nasirian, S. Moayedi, A. Davoudi, and F. L. Lewis, "Distributed cooperative control of DC microrgids," *IEEE Trans. Power Electron.*, vol. 30, no. 4, pp. 2288–2303, Apr. 2015.

[17] S. Moayedi and A. Davoudi, "Distributed tertiary control of DC microgrid clusters," *IEEE Trans. Power Electron.*, vol. 31, no. 2, pp. 1717–1733, 2016.

[18] ——, "Cooperative power management in DC microgrid clusters," in *IEEE 1st Int. Conf. Direct Curr. Microgrids (ICDCM)*, Atlanta, Georgia, June 2015, pp. 75–80.

[19] V. Nasirian, A. Davoudi, and F. L. Lewis, "Distributed adaptive droop control for DC microgrids," in *IEEE Appl. Power Electron. Conf. Expo. (APEC)*, Fort Worth, TX, USA, Mar. 2014, pp. 1147–1152.

[20] M. S. Sadabadi, A. Karimi, and H. Karimi, "Fixed-order decentralized/distributed control of islanded inverter-interfaced microgrids," *Control Engineering Practice*, vol. 45, pp. 174–193, Dec. 2015.

[21] M. Babazadeh and H. Karimi, "A robust two-degree-of-freedom control strategy for an islanded microgrid," *IEEE Trans. Power Del.*, vol. 28, no. 3, pp. 1339–1347, Jul. 2013.

[22] A. H. Etemadi, E. J. Davison, and R. Iravani, "A generalized decentralized robust control of islanded microgrids," *IEEE Trans. Power Syst.*, vol. 29, no. 6, pp. 3102–3113, Nov. 2014.

[23] A. H. Etemadi, E. J. Davison, and R. Iravani, "A decentralized robust control strategy for multi-DER microgrid-Part I: Fundamental concepts," *IEEE Trans. Power Del.*, vol. 27, no. 4, pp. 1843–1853, Oct. 2012.

[24] H. Karimi, E. J. Davison, and R. Iravani, "Multivariable servomechanism controller for autonomous operation of a distributed generation unit: Design and performance evaluation," *IEEE Trans. Power Syst.*, vol. 25, no. 2, pp. 853–865, May 2010.

[25] S. Riverso, F. Sarzo, and G. Ferrari-Trecate, "Plug-and-play voltage and frequency control of islanded microgrids with meshed topology," *IEEE Trans. Smart Grid*, vol. 6, no. 3, pp. 1176–1184, May 2015.

[26] M. S. Sadabadi, Q. Shafiee, and A. Karimi, "Plug-and-play voltage stabilization in inverter-interfaced microgrids via a robust control strategy strategy," *IEEE Trans. Control Syst. Technol.*, Jul. 2016. [Online]. Available: http://ieeexplore.ieee.org/stamp/stamp.jsp?arnumber=7511679

[27] M. Tucci, S. Riverso, J. C. Vasquez, J. M. Guerrero, and G. Ferrari-Trecate, "A decentralized scalable approach to voltage control of DC islanded microgrids," *IEEE Trans. Control Syst. Technol.*, vol. 24, no. 6, pp. 1965–1979, Nov. 2016.

[28] "IEEE recommended practice for monitoring electric power quality, IEEE standard 1159," 2009.

[29] J. Mahdavi, A. Emadi, and H. A. Toliyat, "Application of state space averaging method to sliding mode control of PWM DC/DC converters," in *IEEE Industry Applications Society- Annual Meeting*, New Orleans, Louisiana, Oct. 1997.

[30] V. Venkatasubramanian, H. Schattler, and J. Zaborszky, "Fast time-varying phasor analysis in the balanced three-phase large electric power system," *IEEE Trans. Automat. Control*, vol. 40, no. 11, pp. 1975–1982, Nov. 1995.

[31] R. C. L. F. Oliveira, M. C. de Oliveira, and P. L. D. Peres, "Robust state feedback LMI methods for continuous-time linear systems: Discussions, extensions and numerical comparisons," in *Proc. IEEE Int. Symp. Comp. Cont. Syst. Design (CACSD)*, Denver, CO, USA, 2011, pp. 1038–1043.

[32] M. S. Sadabadi and A. Karimi, "Fixed-order H_∞ and H_2 controller design for continuous-time polytopic systems: An LMI-based approach," in *European Control Conference (ECC13)*, Zurich, Switzerland, July 2013, pp. 1132–1137.

[33] ——, "Fixed-order control of LTI systems subject to polytopic uncertainties via the concept of strictly positive realness," in *American Control Conference (ACC)*, Chicago, IL, July 2015, pp. 2882–2887.

[34] T. Dragicevic, J. M. Guerrero, J. C. Vasquez, and D. Skrlec, "Supervisory control of an adaptive-droop regulated DC microgrid with battery management capability," *IEEE Trans. Power Electron.*, vol. 29, no. 2, pp. 695–706, Feb. 2014.

[35] J. Löfberg, "YALMIP: A toolbox for modeling and optimization in MATLAB," in *Proc. IEEE Int. Symp. Comp. Cont. Syst. Design (CACSD)*, 2004. [Online]. Available: http://control.ee.ethz.ch/~joloef/yalmip.php

[36] MOSEK ApS, *The MOSEK optimization software*, 2011. [Online]. Available: http://www.mosek.com